JOURNAL OF OPTOELECTRONICS AND ADVANCED MATERIALS Vol. 8, No. 6, December 2006, p. 1979 - 1988

Light-induced structural changes in hydrogenated amorphous silicon

T. A. ABTEW*, D. A. DRABOLD*
Department of Physics and Astronomy, Ohio University, Athens Ohio 45701, USA

A direct *ab initio* calculation of network dynamics and diffusion both for the ground state and light excited state for a-Si:H was performed. In the light excited state there was observed enhanced hydrogen diffused and formation of new silicon dihydride configurations: (H-Si Si-H)$_2$(H-Si Si-H) and SiH_2. For the first time, we show the detailed dynamic pathways that arise from light induced occupation changes, and provide one explicit example of defect creation and paired H formation.

(Received October 27, 2006; accepted November 2, 2006)

Keywords: a+Si:H, Light-induced structural changes, Network dynamics

1. Introduction

It is our privilege to submit this paper in honor of Prof. Radu Grigorovici, an important pioneer in the physics of condensed matter. Perhaps this work on light-induced effects in a-Si:H is suited to this volume, as this has been an area of Prof. Grigorovici's interest (his most recent scientific publication in 2002 [1] was on a-Si). His influential work advocating continuous random network models is now the basis of almost every serious modeling study of disordered systems [2]. We are honored indeed to submit this paper in celebration of a remarkable life of 95 years, and we fondly hope for many more.

The demand for improved materials for applications is steadily increasing. These days, there is a huge demand for energy and a need for alternative energy sources. One of these energy sources is solar photovoltaic (PV). Current PV production is entering the gigawatt regime, so a factor of the order 10^3 is needed in order to impact the (terawatt scale) energy markets [3]. One material used for PV energy production is hydrogenated amorphous silicon (a-Si:H), which is particularly inexpensive and serves an important niche in energy markets. An impediment to the use of a-Si:H cells is the so called Staebler-Wronski effect (SWE) [4] (the light-induced creation of carrier traps causing reduced energy conversion efficiency). A salient feature of a-Si:H is that exposure to intense light (as in PV applications) leads to structural change (rearrangements of the positions of the atoms in the amorphous network) [5]. These changes have a serious impact on the performance of a-Si:H cells (the PV efficiency drops 15%-20%, and then stabilizes).

In 1977 Staebler and Wronski reported an experiment on hydrogenated amorphous silicon (a-Si:H) [4], which revealed a marked change in dark photoconductivity after light soaking. Subsequent work showed that defects, most probably dangling bonds, were created by light soaking. Because hydrogenated amorphous silicon (a-Si:H) is a material with technological applications, understanding the phenomenon of light-induced degradation, now named the Staebler-Wronski effect (SWE), has been a major focus.

In the intervening thirty years, extensive work in experiment and modeling has been carried out to obtain the microscopic origin and fundamental understanding of light-induced degradation. Disorder in the network, hydrogen concentration and its complex bonding structure and concentration of impurities are some of the material properties that play a role in the SWE. Such light-induced structural changes are complex and information about the changes is provided by an array of experiments [6, 7]. Key experimental facts are: (1) Light-soaking induces large changes in photoconductivity, and defect (carrier trap) formation; (2) light induces H motion [8, 9] (3) light soaking preferentially creates protons separated by 2.3 Å in device grade material and a shorter distance in low quality material [10], (4) Isoya and coworkers [11] showed that no dangling bond (DB) pairs (adjacent DBs) formed after light soaking and that the placement of the light induced dangling bonds was random [12]. Further, it was shown that metastable dangling bonds were separated by at least 10 Å, (5) studies of defect creation and annealing kinetics in a-Si/Ge:H suggest that there is not a large population of mobile H leading to recapture events of H onto DBs as part of the photo-degradation process [13].

There have been various proposals for the microscopic origins of the SWE. One class of models involves breaking of "weak bonds" which were often unspecified [14]. Another class of models propose the creation of new defects as a result of movement of the original defect [15]. Zafar *et al.* [16] considered a metastability model based on transfer of H between clustered and isolated phases seen by NMR. Bonding in each of these phases was presumed to be monohydride. In their subsequent work Zafar *et al.* [17] showed that the 2-phase picture satisfactorily accounted for new experiments

on the thermal changes in the spin-density and also the changes caused by evolving hydrogen. Nevertheless, this model was unable to account for light-induced effects.

Some current theories combine the electronic and hydrogen energy states and hydrogen diffusion as in the hydrogen collision model of Branz [8] and the hydrogen flip model of Biswas *et al.* [18]. Kopidakis *et al.* [19] proposed that clustered-phase sites can bind either one or two hydrogen pairs (dihydride-bonding). In this line of argument, Zhang *et al.* [20] proposed a model that *m* vacancies of *m* missing Si atoms, provide the H-pair reservoir and metastability sites in Si. There are also recent findings [21] that reveal a lack of spatial correlation between the defects and hydrogen, the realization that the effectiveness of light induced defects as recombination centers depends on the light exposure conditions, and the observation that it is not only defects which are produced by extended light exposure but also larger structural changes in the material involving the Si network.

A clue of importance was recently reported by T. Su *et al.* [22], who performed nuclear magnetic resonance (NMR) experiments on protons in a-Si:H and found that the NMR spectrum of light-soaked a-Si:H films show the preferential creation of a H-H distance of 2.3±0.2 Å. Remarkably, this experiment directly connects light soaking to creation of a specific new structure (or family of structures) in the amorphous matrix. There are two possible interpretations of the results of Su *et al.* [22]. The simplest interpretation is that some metastable, paired-hydrogen site, perhaps, but not necessarily SiH_2, is formed after the exposure to light. A second interpretation, which can not be ruled out by the experiments to date, is that some changes in the various NMR relaxation rates after exposure to light allow existing paired-hydrogen sites, such as SiH_2, to become observable in the NMR spectra. Of particular importance to the latter interpretation, Stutzmann *et al.* [14] have argued that the breaking of weak Si-Si bonds will also promote the diffusion of dangling bonds away from the original site. If the presence of such a dangling bond near a stable, paired-hydrogen site, for which the most logical candidate is SiH_2, allows this site to be seen in the H NMR, then the results of Su *et al.* are also logically explained. Although there are technical reasons why this explanation is not as probable as the formation of metastable, paired-hydrogen sites, it cannot be ruled out.

The experimental results of Su *et al.*[22] pose important questions. Is the observation of two protons separated by a distance of 2.3 Å feasible in terms of the energetics, chemistry and structure of the amorphous network? Since the feature appears to be experimentally robust, it seems likely that a well-defined structure should be associated with it. Finally, if there *are* suitable minimum energy candidate structures, what creates the structure in the first place? In the next section we answer the first question by investigating different structural units and compare them with experiment [23]. The rest of the paper is concerned with an attempt to answer the remaining questions.

2. The feasibility of silicon dihydride structure for the observed NMR experiment

One of the possible candidates for the experimental observation of two protons separated by a 2.3 Å is a dihydride structure. This dihydride structure may be in the form of two H atoms connected to a single Si atom to form a H-Si-H structure where the Si atom is bonded with two additional Si atom and being four coordinated; or two nearby H atoms each connected to a Si atom as Si-H H-Si where each of the Si atoms are bonded with three more Si atoms.

2.1 Models

A predictive simulation requires a physically plausible model that represents the topology of the network and yields an accurate description for dynamics of the atoms. In this article we have used four different supercell models: a 70 atom a-Si:H model (Model-I), a 72 atom a-Si:H model (Model-II), a 71 atom a-Si:H model (Model-III), and a 223 atom a-Si:H model (Model-IV). These models are generated from a 64 atom and a 216 atom a-Si models, which were generated by Barkema and Mousseau [24] using an improved version of the Wooten, Winer, and Weaire (WWW) algorithm [25].

Throughout this paper we use the powerful local basis density functional code SIESTA [26]. This code offers both flexibility and high accuracy, attributes required for studies of disordered phases of matter. A defect-free 64 atom a-Si model [24] is used as a starting configuration for the first three models. Foe Model-I, the working supercell is obtained by removing two Si atoms. The dangling bonds are terminated by adding 8 H atoms to create defect-free (that is, gap state free) structures with SiH_2 structural unit present in the network. This yields a 70 atom a-Si:H Model-I. Model-II is obtained in the same way except that one more Si atom is removed to form a 72 atom a-Si:H (61 Si atoms and 11 H atoms), which includes one dangling bond [27]. We then repeated this supercell surgery at other sites to generate an ensemble of models to obtain some insight into the bonding statistics of SiH_2 conformations in the solid state. The SiH_2 confirmations obtained in the two models are shown in Fig. 1(a) and Fig. 1(b).

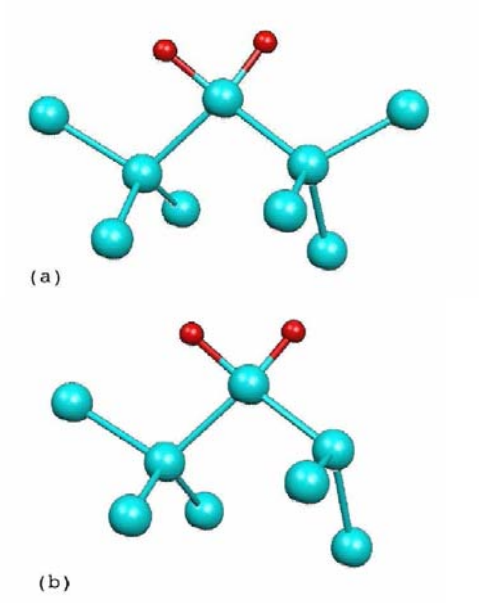

Fig. 1. (a) SiH_2 conformation in Model-I and (b) SiH_2 conformation in Model-II with a dangling bond [23].

To create the a-Si:H environment for Model-III, we removed three silicon atoms resulting in the formation of vacancies. All of the dangling bonds are then terminated by placing a H atom at about 1.5 Å from the corresponding Si atom to generate a 71 atom Model-III. For Model-IV, we started from a 216 atom a-Si model with two dangling bonds, we removed two silicon atoms resulting in the formation of additional vacancies. All of the vacancies except one are then terminated by placing a H atom at about 1.5 Å from the corresponding Si atom. This yields a 223 atom Model-IV. Finally these newly generated structures are well relaxed using conjugate gradient optimization technique. While such a procedure is clearly unphysical, it is worth pointing out that the resulting proton NMR second moments of the clusters created are similar to the broad component of the line shape observed in experiments [28].

2.2 Results

We have considered four configurations for each model in our calculation. Each configuration in the respective models was constructed by selecting different (typically tetrahedral) sites of the SiH_2 conformations in the cell. We performed our calculations of SiH_2 structure and dynamics on each of the four configurations of Model-I and also on each of the four configurations of Model-II. The system was then relaxed using a double zeta polarized (DZP) basis set with a GGA exchange-correlation functional and also repeating the calculation using the same basis and the LDA exchange-correlation functional.

Table 1. The H-H distance before and after relaxation for Model-I using LDA and GGA exchange correlation functional for four different configurations. The GGA (DZP) calculation is expected to be the most accurate [23].

Config--urations	H-H distance before relax--ation (Å)	H-H distance after relaxation (Å)		
		LDA (SZ)	LDA (DZP)	GGA (DZP)
1	1.58	2.51	2.40	2.38
2	2.27	2.38	2.36	2.35
3	3.02	2.69	2.46	2.42
4	3.30	2.59	2.47	2.42
Average		2.54	2.42	2.39

For the first group of four configurations (Model-I), our results are summarized in Table 1. In all these configurations, for different initial proton distances, we see a consistent approach to near the measured proton-proton separation of (2.3±0.2 Å) as the basis set improves from SZ to more complete DZP. Though the shift is smaller, there is also an improvement in going from LDA to GGA functionals. There is a strong message in these results that high-quality calculations are needed to properly describe the structure.

The same calculation has also been done for the Model-II model, and, the results are given in Table 2. As before, a DZP basis set and GGA appears to be necessary. Consistent with the first configuration, Model-II also gives proton separations well within the tolerance of the experiments of Su *et al.* In these results we show that SiH_2 configurations in the solid state are consistent with the experimental observations. We also find that the details of basis set and density functional are important for accurately representing these structures.

Table 2. The H-H distance before and after relaxation for Model-II using LDA and GGA exchange correlation functional for four different configurations. These models contain one dangling bond. The GGA (DZP) calculation is expected to be the most accurate [23].

Config--urations	H-H distance before relax--ation (Å)	H-H distance after relaxation (Å)		
		LDA (SZ)	LDA (DZP)	GGA (DZP)
1	1.61	2.39	2.35	2.34
2	2.20	2.59	2.51	2.46
3	2.35	2.34	2.33	2.32
4	3.29	2.56	2.47	2.44
Average		2.47	2.42	2.39

3. Hydrogen dynamics and its consequences to light exposed a-Si:H

In the previous section, the dihydride structural units are assumed to exist in the network *a priori*, and their

geometry is not inconsistent with the work of Su *et al.*[22]. In the next section we investigate if these dihydride structure units form upon light soaking starting from a network with no dihydride structure in the beginning of the simulation. We have performed extensive MD simulations of network dynamics of a-Si:H both in an electronic ground state ("light-off") and a simulated light-excited state ("light-on") using different models. We present a detailed calculation of hydrogen diffusion, its mechanisms and consequences on the structural electronic and vibrational properties in both electronic ground state and light excited state [5, 29].

3.1 Hydrogen motion: Ground State

To analyze the diffusion mechanism in the ground state we performed a MD simulation for five different temperatures, and tracked the trajectories and bonding information of all the H and Si atoms in the network. In all the cases, the MD simulations show diffusion of hydrogen in the cell and as a consequence, the network exhibits bond breaking and formation processes. The pattern of diffusion differs for individual H atoms depending upon the geometrical constraints around the diffusing H atom.

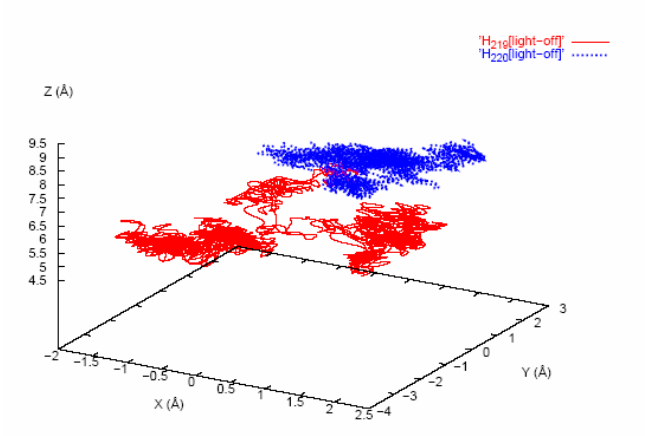

Fig. 2. Trajectory for two different hydrogen atoms (H_{219} and H_{220}) in the ground state, which shows the diffusion and trapping of the atoms for Model-IV. The total time for the trajectory is 10ps [29].

In order to characterize the trajectories of H diffusion in the ground state, we have selected two diffusive H atoms, (H_{219} and H_{220}), and plotted their trajectories at T=300K in Fig. 2. The trajectories for both H_{219} and H_{220} atoms show diffusion in which the H atoms spend time being trapped in a small volume of the cell near a bond center which is followed by rapid emission to another trapping site. In order to examine how the bond rearrangement takes place in the network while the H atom is diffusing, we tracked each hydrogen atoms and computed its bonding statistics.

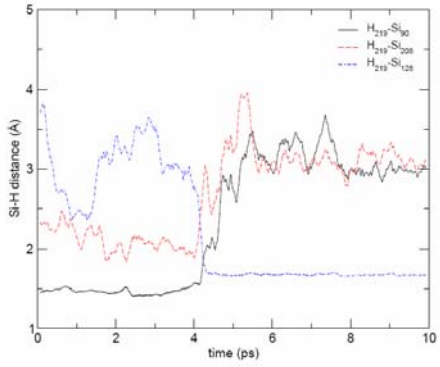

Fig. 3. The Si-H bond length between the diffusing H (H_{219}) and three different Si atoms, (Si_{90}, Si_{208}, and Si_{128} as a function of time in the electronic ground state for Model-IV. The total time for the trajectory is 10ps [29].

In Fig. 3 we show the Si-H bond length between one of the diffusing H atoms (namely H_{219}) and relevant Si atoms (Si_{90} and Si_{128}) with which it forms a bond while diffusing and Si_{208}. As we can see from Fig. 3, in the first 4ps H_{219} is bonded with Si_{90} with a bond length of 1.5 Å and trapped for a while until it breaks and hops to form another bond with Si_{128}. In the first ~4 ps, the bond length between H_{219} and Si_{128} fluctuates between 3.8 Å and 2.5 Å. However, after ~4 ps we observed a swift bond change in a very short period of time ~0.1 ps when the H_{219} atom comes out of the trapping site and hops to form a bond with Si_{128} and becomes trapped there for ~6 ps. This process of trapping and hopping is typical for the highly diffusive H atoms.

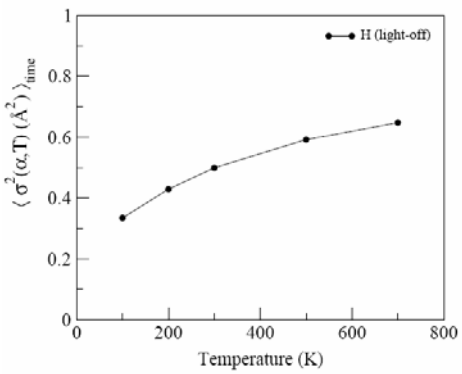

Fig. 4. Time-averaged mean square displacement for H as a function of temperature of MD simulation in electronic ground state for Model-III [29].

To study atomic diffusion we computed the time average mean squared displacement for both H and Si atoms for a given temperature using

$$\left\langle \sigma^2(\alpha,T)\right\rangle_{time} = \frac{1}{N_{MD}N_\alpha}\sum_{t=1}^{N_{MD}}\sum_{i=1}^{N_\alpha}\left|r_i^\alpha(t)-r_i^\alpha(0)\right|^2 \quad (1)$$

where the sum is over particular atomic species α (Si or H), N_α and **Eroare!** are total number and coordinates of the atomic species α at time *t* respectively, and N_{MD} is the

total number of MD steps. The time average mean square displacement for Model-III for five different temperatures was calculated using Eq. 1 for H atoms in the supercell in the electronic ground state ("light-off") and it is shown in Fig. 4. We have observed a strong temperature dependence of H diffusion. This result will help us to compare the diffusion of H in the electronic ground state with the light excited state to be discussed in the next section.

3.2 Excited state dynamics and promotion of carriers

Defects in an amorphous network may lead to localized electron states in the optical gap or in the band tails. If such a system is exposed to band gap light, it becomes possible for the light to induce transitions from the occupied states to unoccupied states. For the present work we do not concern ourselves with the subtleties of how the EM field introduces the transition, we will simply assume that a photo-induced promotion occurs, by depleting the occupied states of one electron "forming a hole" and placing the electron near the bottom of the unoccupied "conduction" states. The idea is that a system initially at equilibrium will not be after the procedure: Hellmann-Feynman forces [30] due to the occupation change will cause structural rearrangements, which may be negligible or dramatic, depending on the flexibility or stability of the network, and the localization of the states. The changes in force will initially be local to the region in which the orbitals are localized, followed by transport of the thermal energy. In general, it is necessary to investigate photo-structural changes arising from various different initial and final states, though only well localized states near the gap have the potential to induce structural change [31-34]. The simulated light excited state is achieved by implementing: a) starting from the well relaxed model, we make the occupation change by adding an additional electron just above the Fermi level, b) we keep the system in this excited state for 10ps (20000 MD steps with time step τ=0.5 fs between each MD steps), and maintain a constant temperature T=300 K, c) after 10ps, we put the system back into the ground state and relax to minimize the energy. The method has been described in additional detail elsewhere [31].

3.3 Hydrogen motion: light excited state

Similar to the case of electronic ground state, we analyzed the diffusion of H in the light excited state by performing a MD simulation. We tracked the trajectories and bonding statistics of Si and H atoms in the supercell. Our MD simulation in the light excited state show enhanced hydrogen diffusion and consequently increased bond breaking and formation that leads to structural changes in the network.

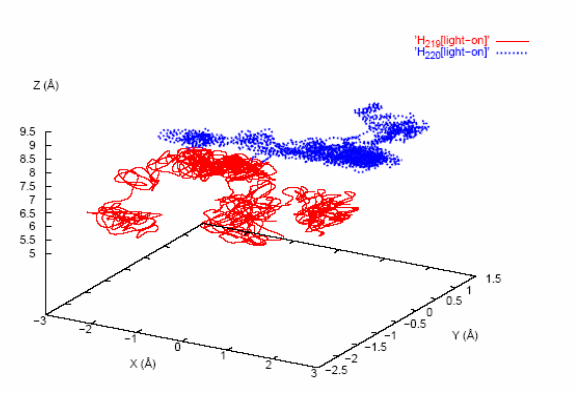

Fig. 5. Trajectory for two different hydrogen atoms (H_{219} and H_{220}) which shows the diffusion and trapping of the atom for Model-IV in the light excited state. The total time for the trajectory is 10ps [29].

For the purpose of analyzing the difference in the diffusion mechanism of H in the light excited state case as compared with the ground state, we performed similar calculations described in the previous sections for the light excited state case. To understand the trajectories of H in the light excited state, we have again selected two diffusive H atoms, (H_{219} and H_{220}) from the larger Model-IV, and plotted their trajectories in the light excited state in Fig. 5. The trajectories show the diffusion of H in the presence of different trapping centers, a region where the H atom spends more time before it hops and moves to another trapping site. However, in this case we observed enhanced diffusion and more trapping sites and hopping. These trapping and hopping processes continue until two hydrogens form a bond to a single Si atom to form a metastable SiH_2 conformation or until two hydrogens form a bond to (a) two different Si atoms which are bonded to each other, to form (H-Si-Si-H) structure or (b) two different Si atoms which are not bonded but close to each other to form (H-Si Si-H) structure. This is in agreement with a basic event of the H collision model [8] and other H-pairing models [19].

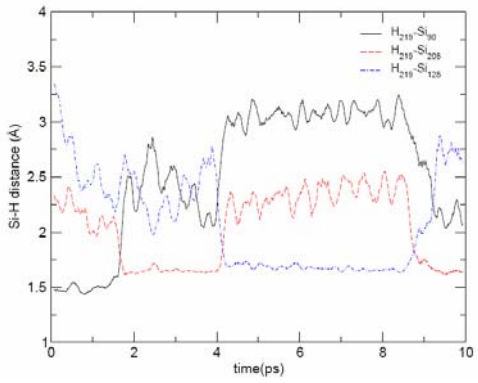

Fig. 6. The Si-H bond length between the diffusing H (H_{219}) and three different Si atoms (Si_{90}, Si_{128}, and Si_{208}) with which H_{219} forms a bond (one at a time) while it is diffusing as a function of time for Model-IV, in the light excited state. The total time for the trajectory is 10 ps [29].

By tracking each H atom, we computed its bonding statistics and examine the bond rearrangements. In Fig. 6 we show Si-H bond length as a function of time between one of the diffusing H atoms (H_{219}) and three other Si atoms (Si_{90}, Si_{128}, and Si_{208}) with which it forms a bond while diffusing in the network. The initial trapping time, where H_{219} is bonded with Si_{90}, is reduced to ~1.8 ps when the light is on from ~4 ps when the light is off. This is followed by another trapping site where H_{219} is bonded with Si_{208} for another ~2.1 ps. The H_{219} hops out of the trapping site and forms a bond with Si_{128} and trapped for ~4.3 ps before it finally hops out from the trapping site and forms another bond with Si_{208} where it gets trapped again and form a silicon dihydride (SiH_2) structure. As we can see from Fig. 6, the pattern of diffusion is quite different from the ground state: In the light excited state case we observed a) more number of trapping sites and less trapping time with frequent hopping, b) enhanced hydrogen diffusion, and c) increasing number of bond rearrangements and newly formed dihydride structural units.

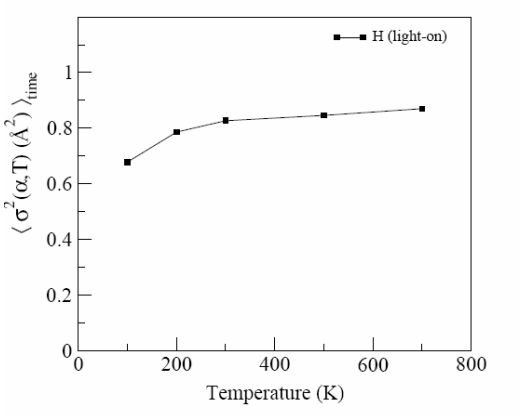

Fig. 7. Time average mean square displacement for H as a function of temperature of MD simulation in the light excited for Model-III [29].

The atomic diffusion in the light excited state case has also been examined using the time average mean squared displacement for both H and Si atoms for different temperatures using Eq. 1 for both Model-IV and Model-III. The results from Model-III are shown in Fig. 7. For all the temperatures considered, our simulation results show enhanced diffusion of Hydrogen for the case when the light is "on" as compared with the case where the light is "off". The enhanced diffusive motion of H in the photo excited state relative to the electronic ground state arises from the strong electron-lattice interaction of the amorphous network, and an effect of "local heating" and subsequent thermal diffusion [32] initially in the spatial volume in which the state is localized. The same calculations has also been performed on the larger model Model-IV at T=300 K in which, the time average mean square displacement for H is 2.66 $Å^2$ for the light excited state and 1.10 $Å^2$ for the electronic ground state. These results again show and confirm enhanced hydrogen diffusion for the light excited state. However, while we have shown that light-induced occupation change can induce H motion, we seen an example without additional diffusion. This emphasizes the need for further work with additional models (and therefore different defect states), and additional studies of the influence of occupation changes involving other states near the gap.

4. Consequences of hydrogen diffusion

4.1 Formation of dihydride structure

In the two scenarios that we considered, MD simulation in electronic ground state (light off) and simulated light-excited state (light on) we have observed an important difference. In the light-excited state, in addition to bond rearrangements and enhanced hydrogen diffusion, we have observed a preferential formation of new structure: SiH_2, with an average distance of 2.39 Å for the pair of hydrogen in the structure, (H-Si-Si-H) and (H-Si Si-H) with H-H separation, which ranges from 1.8 Å to 4.5 Å. However, in the electronic ground state, we have obtained rearrangement of atoms including hydrogen diffusion, without formation of SiH_2 structure in the supercell. The mechanisms for the formation of these structures in the light-excited state follows breaking of H atom from Si-H bond close to the dangling bonds and diffusion to the nearest weakly bonded interstitial sites (or dangling bonds). This mobile H atom then collides (forms a metastable bond) with another Si+DB structure or breaks a Si-Si bond to form another Si-H bond. This is attributed to the fact that the dangling bond site is moving to accommodate the change in force caused by the additional carrier and also because hydrogen is moving through weakly bonded interstitial sites with low activation barrier for diffusion until it is trapped by a defect [35].

In Fig. 8(a)-8(f), we have shown the snapshots [37] taken for intermediate steps in the dynamics of the whole cell, in the presence of charge carrier, where emphasis is given to the two hydrogens, which eventually be part of the SiH_2 conformation. For instance, considering the first configuration of Model-III, the two hydrogens that involved in the formation of the SiH_2 structure initially were about 5.50 Å apart and bonded to two different Si atoms (Si-H) which were separated by about 4.86 Å. Upon MD simulations, the two hydrogen atoms dissociate from their original host and becomes mobile until they form the SiH_2 structure, in which the H-H distance is 2.37 Å which barely changes upon relaxation to 2.39 Å. We have observed similar pattern of H diffusion, bond rearrangements and formation of SiH_2 structure near the db for the other two configurations considered in the simulation. We have summarized the results that show H-H distance (in SiH_2 structure) in Table 3.

We find that there are two different modes of bond formation for the mobile hydrogen. The first is when two mobile hydrogen atoms, H_m, collide with two Si atoms and form a metastable (H-Si-Si-H) or (H-Si Si-H) structure and the second one is when the mobile hydrogen moves until it encounters a preexisting Si-H+DB structure and makes a bond to form a SiH_2 structure.

Consequently, our calculations show two basic ideas for the diffusion of H in the light-excited state: 1) the diffusion of hydrogen doesn't only break a Si-H bond but it also breaks a Si-Si bond and 2) the possibility that two mobile H atoms might form a bond to a single Si atom to form a metastable SiH_2 structure in addition to the formation of (H-Si-Si-H) and (H-Si Si-H) structures.

In Model-III, the two hydrogens involved in the formation of the SiH_2 structure initially were 5.50 Å apart and bonded to two different Si atoms (Si-H), which were separated by 4.86 Å. With thermal simulation in the light excited state, the two hydrogen atoms dissociate from their original Si atoms and become mobile until they form the SiH_2 structure, in which the H-H distance becomes 2.39 Å. We have observed similar pattern of H diffusion, bond rearrangements and formation of SiH_2 structure near the DB for the other two configurations considered in the simulation. The same phenomenon is observed in the case of Model-IV. The two hydrogens involved in the formation of the SiH_2 structure initially were 3.29 Å apart and bonded to two different Si atoms (Si-H), which were separated by 3.92 Å. With thermal simulation in the light excited state, the two hydrogen atoms dissociate from their original host and become mobile until they form the SiH_2 structure, in which the H-H distance becomes 2.45 Å. We have summarized the results that show before and after MD calculations of H-H distance (in SiH_2 structure) for Model-IV and three different configurations of Model-III in the case of light excited state in Table 3.

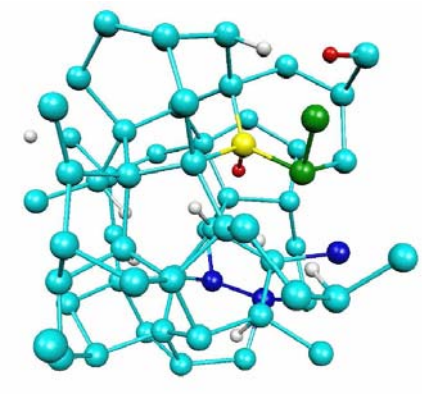

a

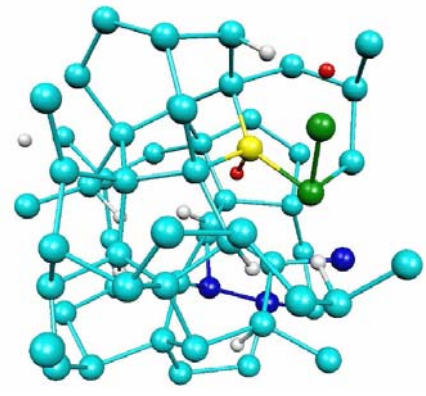

b

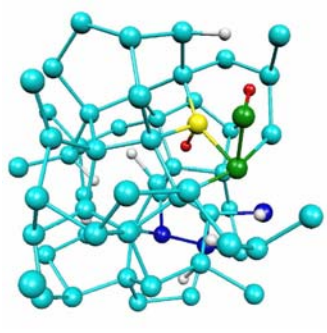

c

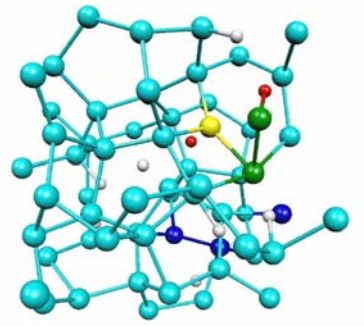

d

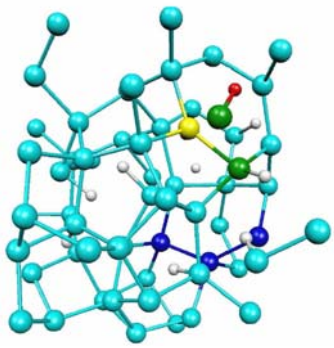

e

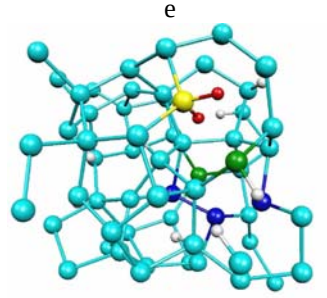

f

Fig. 8. Thermal MD simulation for Model-III in the presence of carriers, which shows an example of SiH_2 formation. a) The initial configuration in which the two hydrogens (that eventually form SiH_2) are initially attached to two different Si atoms forming Si-H bond, b) One of the hydrogens dissociates from Si-H and form mobile hydrogen and leaves a dangling bond, c) the mobile hydrogen forms a bond with another Si(db) atom, d) the other H atom also leaves a dangling bond and becomes mobile, e) rearrangements of bonds near the defect sites, and f) The formed SiH_2 structure after being relaxed to the minimum energy. (The two hydrogens that form the SiH_2 structure are shown in red while the Si atom in this structure is shown in yellow, and also we represent the initial defect sites with green and the final defect sites with blue.) [5].

Table 3. The H-H distance in the SiH_2 configurations of the system before and after MD simulations in the light excited case [29].

Config--urations	H-H distance before MD (Å)	H-H distance after MD (Å)
1 (Model-III)	5.50	2.39
2 (Model-III)	3.79	2.36
3 (Model-III)	4.52	2.36
4 (Model-IV)	3.29	2.45
Average		2.39

4.2 Change in the electronic properties

In order to understand the electron localization we used the inverse participation ratio, *I*,

$$I = \sum_{i=1}^{N} [q_i(E)]^2 \qquad (2)$$

where $q_i(E)$ is the Mulliken charge [37] residing at an atomic site *i* for an eigenstate with eigenvalue *E* that satisfies (2) and *N* is the total number of atoms in the cell. For an ideally localized state, only one atomic site contributes all the charge and so *I*=1. For a uniformly extended state, the Mulliken charge contribution per site is uniform and equals 1/*N* and so *I*=1/*N*. Thus, large *I* corresponds to localized states. With this measure, we observe a highly localized state near and below the Fermi level and a less localized state near and above the Fermi level. These states, highest occupied molecular orbitals (HOMO) and lowest unoccupied molecular orbitals (LUMO), are centered at the two dangling bonds in the initial configuration of the model. The energy splitting between the HOMO and LUMO states is 1.08 eV. Fig. 9 (a) shows the Fermi level and *I* of these two states and other states as a function of energy eigenvalues in the relaxed electronic ground state.

This picture changes when we excite the system and perform a MD calculation in which we observe enhanced diffusion of hydrogen and subsequent breaking and formation of bonds. Since electron-phonon coupling is large for localized states [38], the change of occupation causes the forces in the localization volume associated with the DB to change and the system moves to accommodate the changed force. Consequently, the hydrogen atoms close to the DB sites start to move in the vicinity of these defects either to terminate the old DB's or to break a weak Si-Si bond and by doing so, create new DB defects on nearby sites. As shown in Fig. 9 (b) we observe the formation a highly localized state and appearance of three less localized states, that correspond to the newly formed defect levels after simulated light-soaking. These processes induce transition of electrons from the top of the occupied states to the low-lying unoccupied states, which is reflected in the smaller value of the initial I_{HOMO} and an increase in the I_{LUMO}.

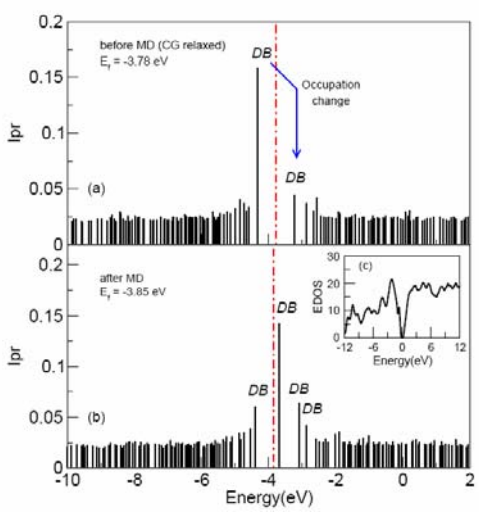

Fig. 9. The inverse participation ratio I of the eigenstates versus the energy eigenvalues, (a) in the relaxed electronic ground state and (b) in the relaxed simulated light-excited state (light excited MD followed by relaxation), with their respective Fermi energy in the first configuration of relaxed Model-III. The inset (c) shows the electron density of states with the Fermi level shifted to zero for the relaxed simulated light-excited state [29].

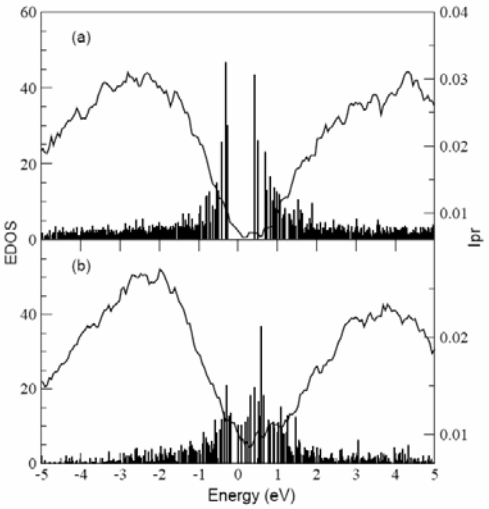

Fig. 10. (Color Online) The energy density of states and the inverse participation ratio I of the eigenstates versus the energy eigenvalues, (a) in the relaxed electronic ground state and (b) in the relaxed simulated light-excited state (light excited MD followed by relaxation), both the electron density of states and the inverse participation ratio are plotted with the Fermi level shifted to zero [29]. Results are for Model IV.

I_{HOMO}, where the state is initially localized, decreases from 0.158 to 0.060 after photo-excitation, while the I_{LUMO} increases from 0.045 to 0.142. The splitting energy between the HOMO and LUMO states has also declined to 0.723 eV. The newly formed defects with lower energy splitting between the HOMO and LUMO states suggest a presence of carrier induced bond rearrangements in the supercell. The comparisons for the energy and *I* of the

system before MD (as relaxed) and after MD is given in Table 4.

Table 4. The energy and the inverse participation ratio I of localized states HOMO, LUMO, LUMO+1 and LUMO+2 before and after the MD for Model-III [29].

	Eigenvalue		I	
	before MD (eV)	after MD (eV)	before MD	after MD
HOMO	-4.32	-4.40	0.158	0.060
LUMO	-3.24	-3.68	0.045	0.142
LUMO+1	-2.88	-3.08	0.037	0.064
LUMO+2	-2.66	-2.87	0.030	0.042

In addition, analysis of the spatial distribution of the configurations shows that the H atoms close to the dangling bonds (< 4.0 Å) are most diffusive and the Si atoms, which make most of the bond rearrangements including the Si atom in the SiH_2 configurations, are close (< 5.50 Å) to the dangling bonds. These show the additional charge carrier induces change in the forces around the dangling bonds and consequently rearranges the atoms around the dangling bond sites and eventually forming a SiH_2 structure. On average the newly formed defect sites are 3.80 Å and 4.70 Å far away from the two initial defect sites. The newly formed SiH_2 structure is (on average) 4.11 Å away from the initial defect sites. It is probable that limitations in both length and time scales influence these numbers, but it is clear that the defect creation is *not* very local because of the high diffusivity of the H.

The same calculation has been performed on Model-IV. In Fig. 10 we have plotted both energy density of states and inverse participation ratio as a function of energy in the light excited state case before and after the MD simulation. As can be seen from the figure we obtained more localized states in the middle of the gap, which are caused due to an increase in the number of defects upon light excitation. This supports that the diffusion of hydrogen not only forms preferential dihydride structures but also increase the number of defects in agreement with our findings for the smaller cell Model-III.

4.3 Change in the vibrational properties

For an amorphous solid, the vibrational density of state is a sum of $3N$ (N is the number of atoms) delta functions corresponding to the allowed frequency modes. Starting with the relaxed Model-III subsequent to MD in the light excited state, we computed the vibrational energies (vibrational modes) from the dynamical matrix, which is determined by displacing each atom by 0.02 Å in three orthogonal directions and then performing *ab initio* force calculations for all the atoms for each displacement to obtain the force constant matrix, and with diagonalization, phonon frequencies and modes.

Table 5. Frequency for some of the Si-H vibrational modes of the SiH_2 conformation for the first two configurations of Model-III obtained from our MD simulations and their corresponding experimental values [29].

Configurations	Rocking cm^{-1}	Scissors cm^{-1}	Stretch cm^{-1}
1	629	810	2025
2	625	706	2047
Experiment[39-41]	630	875	2090

In our calculations, the VDOS shows H modes of vibrations in the range (600-900) cm^{-1} and also in the range (1800-2100) cm^{-1}. We have examined the vibrational modes to pick out those modes arising only from SiH_2. We reproduce the vibrational modes of SiH_2 and their corresponding experimental values [39-41] in Table 5. The first mode is rocking at 629 cm^{-1} and 625 cm^{-1}; in this paper, the second is the scissors mode at 810 cm^{-1} and 706 cm^{-1}. Finally we observe the asymmetric stretching mode at 2025 cm^{-1} and 2047 cm^{-1} for the first and second configurations respectively. These results are in good agreement with the IR absorption spectra for the SiH_2 structure. The comparison of our results for the vibrational modes of SiH_2 with the experiment is summarized in Table 5. The results shown in Table 5 are sensitive to the basis sets used in the calculation, in agreement with other work emphasizing the delicacy of H dynamics [42].

In conclusion, we have presented a direct *ab-initio* calculation of network dynamics and diffusion both for the electronic ground state and light-excited state for a-Si:H. We computed the preferential diffusion pathways of hydrogen in the presence of photo-excited carriers. In the light-excited state, we observe enhanced hydrogen diffusion and formation of new silicon dihydride configurations, (H-Si-Si-H), (H-Si Si-H), and SiH_2. The two hydrogens in the SiH_2 unit show an average proton separation of 2.39 Å. The results are consistent (a) with the recent NMR experiments and our previous studies, and (b) with the hydrogen collision model of Branz and other paired hydrogen model in the basic diffusion mechanism and formation of dihydride structures. In contrast, simulations in the electronic ground state do not exhibit the tendency to SiH_2 formation. Undoubtedly, other H diffusion pathways exist, and the importance of larger simulation length and time scales as well as effects of promotions involving different states (which could include strain defects and floating bonds [43]) should be undertaken. For the first time, we show the detailed dynamic pathways that arise from light-induced occupation changes, and provide one explicit example of defect creation and paired H formation.

Acknowledgments

We thank P. C. Taylor for collaboration and providing much of the initial motivation for undertaking the study. We thank E. A. Schiff and P. A. Fedders for helpful conversations. We acknowledge support from the National Science Foundation and the Army Research Office. Some of this work has appeared elsewhere.

References

[1] R. Grigorovici, M. Popescu, in Physics and Applications of Disordered Materials, M. Popescu, Editor, INOE, Bucharest p. 19 (2002).
[2] R. Grigorovici, R. Manaila, Nature **226**, 142 (1970).
[3] Smalley, R. E. Future global energy prosperity: the terawatt challenge. MRS Bulletin **30**, 412 (2005).
[4] D. L. Staebler, C. R. Wronski, Appl. Phys. Lett. **31**, 292 (1977).
[5] T. A. Abtew, D. A. Drabold, J. Phys.: Condens. Matt. **18**, L1 (2006).
[6] Fritzsche, H. Light-Induced Structural Changes in Glass, in Insulating and Semiconducting Glasses p653, (World Scientific, Singapore, 2000).
[7] Singh, J. & Shimakawa, K. Advances in Amorphous Semiconductors Ch. 10 (Taylor and Francis, London, 2003).
[8] H. M. Branz, Sol. St. Comm. **105/6**, 7725 (1999); Phys. Rev. B **74**, 085201 (2006).
[9] H. M. Cheong, S. H. Lee, B. P. Nelson, A. Mascarenhas, App. Phys. Lett. **77**, 2686 (2000).
[10] T. Su, P. C. Taylor, G. Ganguly, D. E. Carlson, Phys. Rev. Lett. **89**, 015502 (2002).
[11] J. Isoya, S. Yamasaki, H. Ohushi, A. Matsuda, K. Tanaka, Phys. Rev. B **47**, 7013 (1993).
[12] S. Yamasaki, J. Isoya, J. Non. Cryst. Sol. **166**, 169 (1993).
[13] K. C. Palinginis, J. D. Cohen, S. Guha, J. C. Yang, Phys. Rev. B **63**, 201203 (2001).
[14] M. Stutzmann, W. B. Jackson, C. C. Tsai, Phys Rev B **32**, 23 (1985).
[15] R. Biswas, I. Kwon, C. M. Soukoulis, Phys. Rev. B **44**, 3403 (1991).
[16] S. Zafar, E. A. Schiff, Phys. Rev. B **40**, 5235 (1989).
[17] S. Zafar, E. A. Schiff, Phys. Rev. Lett. **66**, 1493 (1991).
[18] R. Biswas, Y. -P. Li, Phys. Rev. Lett. **82**, 2512 (1999).
[19] N. Kopidakis, E. A. Schiff, J. Non. Cryst. Solids **266-269**, 415 (2000).
[20] S. B. Zhang, H. Branz, Phys. Rev. Lett. **87**, 105503 (2001).
[21] H. Fritzsche, Annu. Rev. Mater. Res. **31**, 47-79 (2001).
[22] T. Su, P. C. Taylor, G. Ganguly, D. E. Carlson, Phys. Rev. Lett. **89**, 015502 (2002).
[23] T. A. Abtew, D. A. Drabold, P. C. Taylor, Appl. Phys. Lett. **86**, 241916 (2005).
[24] J. M. Soler, E. Artacho, J. D. Gale, A. Garcia, J. Junquera, P. Ordejon, D. Sanchez-Portal, J. Phys. Cond. Matter **14,** 2745 (2002).
[25] G. T. Barkema, N. Mousseau, Phys. Rev. B **62**, 4985 (2000).
[26] F. Wooten, K. Winer, D. Weaire, Phys. Rev. Lett. **54**, 1392 (1985).
[27] This second conformation reveals only that the proton-proton distances reported are “robust" even for a rather different chemical environment. It is unlikely that the SiH_2 would be so close to a dangling bond. See S. Yamasaki, H. Okushi, A. Matsuda, K. Tanaka, J. Isoya, Phys. Rev. Lett. **65**, 756 (1990).
[28] P. A. Fedders, D. A. Drabold, Phys. Rev. B **47**, 13277 (1993).
[29] T. A. Abtew, D. A. Drabold, Phys. Rev. B **74**, 085201 (2006).
[30] R. P. Feynman, Phys. Rev. **56**, 340 (1939).
[31] P. A. Fedders, Y. Fu, D. A. Drabold, Phys. Rev. Lett. **68**, 1888 (1992); D. A. Drabold, S. Nakhmanson, X. Zhang, in Proceedings of NATO advanced study institute on Properties and applications of amorphous materials, Czech Republic, 2001 edited by M. F. Thorpe and L. Tichy (Kluwer, London, 2001), p. 221.
[32] X. Zhang, D. A. Drabold, Phys. Rev. Lett. **83**, 5042 (1999).
[33] X. Zhang, D. A. Drabold, Intl. J. Mod. Phys. **15**, 3190 (2001).
[34] J. Li, D. A. Drabold, Phys. Rev. Lett. **85**, 2785 (2000).
[35] P. V. Santos, W. B. Jackson, Phys. Rev. B **46**, 4595 (1992).
[36] MOLEKEL 4.0, P. Flükiger, H. P. Lüthi, S. Portmann, and J. Weber, Swiss Center for Scientific Computing, Manno (Switzerland) (2000).
[37] A. Szabo, N. S. Ostlund, Modern Quantum Chemistry, (McGraw-Hill, New York, 1989), p. 151.
[38] R. Atta-Fynn, P. Biswas, D. A. Drabold, Phys. Rev. B **69**, 245204 (2004).
[39] M. H. Brodsky, Manuel Cardona, J. J. Cuomo, Phys. Rev. B **16**, 3556 (1977).
[40] G. Lucovsky, R. J. Nemanich, J. C. Knights, Phys. Rev. B **19**, 2064 (1979).
[41] W. P. Pollard, G. Lucovsky, Phys. Rev. B **26**, 3172 (1982).
[42] C. G. Van de Walle, Phys. Rev. B **49**, 4579 (1994).
[43] D. A. Drabold, P. A. Fedders, O. F. Sankey, J. D. Dow, Phys. Rev. B **42**, 5135(1990).

*Corresponding authors: abtew@phy.ohiou.edu, drabold@ohio.edu